

FEDSM-ICNMM2010-1000*

LOSS COEFFICIENTS IN LAMINAR FLOWS: INDISPENSABLE FOR THE DESIGN OF MICRO FLOW SYSTEMS

H. Herwig, B. Schmandt, M.-F. Uth

Institute of Thermo-Fluid Dynamics, Hamburg University of Technology, 21073 Hamburg, Germany

ABSTRACT

The concept of head loss coefficients K for the determination of losses in conduit components is discussed in detail. While so far it has mainly been applied to fully turbulent flows it is extended here to also cover the laminar flow regime. Specific numbers of K can be determined by integration of the entropy generation field (second law analysis) obtained from a numerical simulation. This general approach is discussed and illustrated for various conduit components.

Keywords: second law analysis, head loss coefficient, entropy generation rates, conduit components, upstream/downstream length, laminar flow, numerical simulation

p_i	m	cell centre coordinate
P_{loss}	W	power loss
r	m	radius
R	J/kgK	gas constant
Re	—	Reynolds number
s_c	m	centerline coordinate
\dot{S}_D	W/K	entropy generation rate by dissipation
T	K	Temperature
u, v, w	m/s	velocity components
u_m	m/s	mean velocity
V	m ³	volume of the conduit
y	m	coordinate in direction of g

NOMENCLATURE

C_i	—	constants
D_h	m	hydraulic diameter
f	—	friction factor
g	m/s ²	gravitational acceleration
K	—	head loss coefficient, equation (1)
K_E	—	exergy loss coefficient, equation (15)
L_u, L_d	m	upstream/downstream length
N	—	number
p	Pa	pressure

Greek letters

ϕ	J/kg	specific dissipation
ν	m ² /s	kinematic viscosity
μ	kg/ms	dynamic viscosity
ρ	kg/m ³	density

Subscripts and superscripts

\square'	1/m	value per length
\square'''	1/m ³	value per volume
\square°		undisturbed flow
\square_c		within a component
\square_d		downstream
\square_u		upstream

□_∞

ambient conditions

INTRODUCTION

It is common practice in the design of flow systems to account for losses in total head (and thus mechanical energy) by the use of *head loss coefficients* K . These coefficients characterize single components like bends, trijunctions, nozzles, diffusers and the like with respect to the loss of total head associated with them.

The general definition of K is

$$K \equiv \frac{2\varphi}{u_m^2} \quad (1)$$

with $\varphi = P_{\text{loss}}/\dot{m}$ as specific dissipation, i.e. the power lost by dissipation (P_{loss}) referred to the mass flux (\dot{m}). Since $u_m^2/2$ is the specific kinetic energy (i.e. the kinetic energy per mass m), K actually is the ratio of the dissipated and the kinetic energy in a conduit component.

The specific dissipation φ_{12} associated with the flow between two cross sections (1) and (2) explicitly appears in the mechanical energy equation of a one-dimensional flow model (BERNOULLI equation). For incompressible flow this equation reads (see e.g. [3]):

$$\alpha_1 \frac{u_{m1}^2}{2} + \frac{p_1}{\rho} + gy_1 = \alpha_2 \frac{u_{m2}^2}{2} + \frac{p_2}{\rho} + gy_2 + \varphi_{12} \quad (2)$$

with

$$\alpha_i = \frac{1}{u_{mi}^3 A_i} \int u_i^3 dA_i \quad (3)$$

Here α_i takes into account how u_i is distributed over the cross section with $\alpha_i = 1$ for $u_i = u_m$ (one dimensional approximation) and $\alpha_i = 2$ for a parabolic u_i -profile, for example.

From equation (2) we get

$$\varphi_{12} = \frac{p_1 - p_2}{\rho} + \frac{\alpha_1 u_{m1}^2 - \alpha_2 u_{m2}^2}{2} + g(y_1 - y_2) \quad (4)$$

From equation (4) it is obvious that φ_{12} corresponds to the pressure drop when $\alpha_1 u_{m1}^2 = \alpha_2 u_{m2}^2$ and $y_1 = y_2$, i.e. when the flow is neither accelerated nor decelerated and when the flow is horizontal so that there is no change in potential energy. Only then (and not in general) K alternatively can be written as

$$K = \frac{2\Delta p}{\rho u_m^2} \quad (\text{only for } \Delta(\alpha u_m^2) = 0, \Delta y = 0) \quad (5)$$

So far no assumption has been made about the flow status, i.e. whether the flow is laminar or turbulent. For fully turbulent flows some numbers K are tabulated in almost all standard fluid mechanics text books like [1], [2] and [3]. Comprehensive collections of K -numbers can be found in [4] and [5], for example. These data, however, are applicable for fully turbulent flows only. In micro-flow devices the flow almost always is laminar and a new look to the K -concept is required.

Before this is done in our study, it is illustrative to investigate quite generally for which cases K according to its definition (1) is a constant value and for which it is not. In a nondimensional theory this corresponds to the question, how K depends on the Reynolds number $\text{Re} = u_m D_h / \nu$.

THE K-VALUE AND ITS Re-DEPENDENCE

Instead of equation (2), which is a one-dimensional simplification (model), the NAVIER-STOKES equations are considered. From a continuum point of view, they basically are NEWTON's second law applied to an infinitesimal mass $dm = \rho dV$ and thus constitute the balance of forces with respect to dm . Forces involved are inertia forces, pressure forces, buoyancy forces and "friction forces" F , which are due to dissipation. For internal flows these friction forces F correspond to the nominator in the definition of K see equation (1) and equation (5), respectively. Thus, with a constant, not fixed with respect to its specific number, K is proportional to F/u_m^2 , i.e.

$$K = \text{const} \frac{F}{u_m^2} \quad (6)$$

According to this equation, K is a constant only for $F \propto u_m^2$. In all other cases K depends on u_m , which in a nondimensional theory corresponds to a Reynolds number dependence of K .

For a general discussion of conduit components and straight channels let us assume

$$F \propto u_m^n \quad \text{with } 1 \leq n \leq 2 \quad (7)$$

so that

$$K \propto \text{Re}^{n-2} \quad (8)$$

Table 1. REYNOLDS NUMBER DEPENDENCE OF THE K-VALUE DEDUCED FROM A GENERAL BALANCE OF FORCES; S: SMOOTH, R: ROUGH

		Re:	low	moderate	high	very high
comp.	lam		Re^{-1}	Re^{n-2}	const	—
	turb		—	Re^{n-2}	const	const
channel	lam	s	Re^{-1}	Re^{-1}	Re^{-1}	—
		r	Re^{-1}	Re^{-1}	Re^{n-2}	—
	turb	s	—	Re^{n-2}	Re^{n-2}	Re^{n-2}
		r	—	Re^{n-2}	Re^{n-2}	const

In the common notation of the NAVIER-STOKES equations inertia forces appear on the left hand side, where the only non-linear terms are (assuming constant properties for the moment). As a consequence, inertia forces are nonlinear forces ($\propto u_m^2$) and the force balance will result in a friction force $F \propto u_m^n$ with $n \neq 1$ whenever forces appear in the balance that come from the left hand side of the NAVIER-STOKES equations. In laminar flows these are the inertia forces themselves, in turbulent flows, however, these are also all turbulent force components since the additional turbulent terms in the equations all stem from the non-linear terms on the left hand side.

With these considerations we can distinguish three options for n which are all found in table 1, where Reynolds numbers are characterized as low, moderate, high and very high with “low” excluded for turbulent flow and “very high” for laminar flow. Since straight channels may also be components in a system they are included. They need, however, an extra treatment since in channels wall roughness may have a strong influence (see [6] for further details). The three options are:

(1) $n = 1$, i.e. $K \propto Re^{-1}$:

The left hand side of the NAVIER-STOKES equations vanishes completely. This is the case

- for conduit components when the flow is laminar with $u_m \rightarrow 0$, which then is a *creeping flow* (low Reynolds number)
- for straight channels with smooth walls when the flow is laminar with $grad u_m = 0$, which then is a *fully developed flow*, or with rough walls but only for low and moderate Reynolds numbers.

(2) $n = 2$, i.e. $K \propto Re^0 = \text{const}$:

The inertia forces dominate and thus are effectively the only forces in balance with F . This is the case

- for conduit components when the flow is laminar with high Reynolds numbers or when the flow is fully turbulent with high or very high Reynolds numbers
- for straight channels with rough walls and very high Reynolds numbers when the flow is turbulent (then inertia forces around the roughness elements predominate, although the flow is fully developed in the mean).

(3) $1 < n < 2$, i.e. $K \propto Re^{n-2}$:

Inertia forces are present together with other forces. This is the case

- for conduit components with moderate Reynolds numbers
- for straight channels with smooth walls when the flow is turbulent at arbitrary Reynolds numbers or, with rough walls when the flow is turbulent but at moderate or high Reynolds numbers, or with very rough walls when the flow is laminar at high Reynolds numbers.

The Reynolds number dependence of K for the laminar case is the basis for the new look to the K -concept when flows are laminar, see table 1.

THE K-CONCEPT FOR LAMINAR FLOWS

The first line in table 1 shows that for laminar flow in conduit components the Reynolds number dependence occurs with an exponent that is -1 for low Re and increases to 0 when Re gets larger. This corresponds to the absence of inertia forces for low Re and their increasing importance when Re gets larger.

With these two limits, i.e.

$$K \propto Re^{-1} \quad \text{for } Re \rightarrow 0; \quad K \propto Re^0 \quad \text{for } Re \rightarrow \infty \quad (9)$$

we may tentatively assume that K has the general form

$$K \equiv \frac{2\varphi}{u_m^2} = C_1 + C_2/Re \quad (10)$$

Following Churchill and Usagi [7] for a more sophisticated formula that incorporates two asymptotes we may also assume

$$K \equiv \frac{2\varphi}{u_m^2} = \left[\hat{C}_1^m + (\hat{C}_2/Re)^m \right]^{1/m} \quad (11)$$

with $m = 1$ reducing equation (11) to equation (10).

In order to determine K and then find C_1 and C_2 or \hat{C}_1 , \hat{C}_2 and m , respectively, we have to determine φ , which is the *specific dissipation associated with the flow through the component* under consideration. It is important to note, that it is not the *specific dissipation in the component*, since certain amounts of φ will be found in the upstream and downstream parts of the flow field adjacent to the component itself.

Therefore we divide φ into three parts

$$\varphi \equiv \Delta\varphi_u + \varphi_c + \Delta\varphi_d \quad (12)$$

with:

- $\Delta\varphi_u$: additional specific dissipation upstream
- φ_c : specific dissipation within a component
- $\Delta\varphi_d$: additional specific dissipation downstream

What also is important to know is how far upstream and downstream the impact of a component is felt in the flowfield. This can be expressed in terms of an upstream and downstream *length of impact*. We define them as those lengths L_u and L_d within which 95% of the additional specific dissipation occurs, i.e.:

$$L_u : \text{upstream length with } 0.95\Delta\varphi_u \quad (13)$$

$$L_d : \text{downstream length with } 0.95\Delta\varphi_d \quad (14)$$

With the hydraulic diameter D_h as a characteristic length, a component can thus be characterized by the following table 2 with respect to the details of losses in a laminar flow.

Table 2. DETAILED INFORMATION ABOUT LOSSES DUE TO A CONDUIT COMPONENT FOR N DIFFERENT REYNOLDS NUMBERS

Re	$\Delta\varphi_u/\varphi$	φ_c/φ	$\Delta\varphi_d/\varphi$	L_u/D_h	L_d/D_h	K
	eqn. (12)	eqn. (12)	eqn. (12)	eqn. (13)	eqn. (14)	eqn. (1)
Re ₁
⋮	⋮	⋮	⋮	⋮	⋮	⋮
Re _N

From the values for $K = K(\text{Re})$ in the last column of table 2 the constants C_1 and C_2 or \hat{C}_1 , \hat{C}_2 and m in equation (10) and equation (11), respectively, can be determined by fitting the general ansatz to the data of this table.

THERMODYNAMIC CONSIDERATIONS

Losses in a flow field occur due to the dissipation of mechanical energy by the viscous (in the turbulent case: also turbulent) flow. From a thermodynamic point of view this dissipation is a conversion of mechanical energy into thermal (internal) energy. If this happens at environmental temperature T_∞ this also is a corresponding conversion of exergy (available work) into energy, accompanied by the generation of entropy. On the temperature level T_∞ the loss of total head exactly corresponds to the loss of exergy.

If dissipation φ happens on a temperature level $T \neq T_\infty$, however, the situation is different. For $T > T_\infty$, for example, the dissipated mechanical energy is not completely lost exergy since the (additional) internal energy now, due to $T > T_\infty$, has a certain exergy fraction. Then K according to equation (1) quantifies the head loss, but not the exergy loss, which from a thermodynamic point of view is the “true” loss.

Therefore, we suggest to define an *exergy loss coefficient* K_E which can be determined by integration of the local entropy generation as will be demonstrated hereafter. Its definition is

$$K_E \equiv \frac{T_\infty \dot{S}_D / \dot{m}}{u_m^2} \quad (15)$$

with \dot{S}_D being the overall entropy generation due to the conduit component.

For an isothermal situation at T_∞ , the exergy loss coefficient K_E is equal to K according to equation (1) and thus K can be determined like K_E for $T = T_\infty$.

HOW TO DETERMINE K_E and K

The entropy generation in a flow field is a direct measure of the exergy losses and therefore can be used to determine K_E according to equation (15). Assuming $T = T_\infty = \text{const}$ this also gives K according to equation (1). For the general background of this *second law analysis* (second law of thermodynamics) see e.g. [8] and [9].

In a laminar flow field the local entropy generation rate in cartesian coordinates is (see [10])

$$\begin{aligned} \dot{S}_D''' = \frac{\mu}{T} & \left(2 \left[\left(\frac{\partial u}{\partial x} \right)^2 + \left(\frac{\partial v}{\partial y} \right)^2 + \left(\frac{\partial w}{\partial z} \right)^2 \right] \right. \\ & \left. + \left(\frac{\partial u}{\partial y} + \frac{\partial v}{\partial x} \right)^2 + \left(\frac{\partial u}{\partial z} + \frac{\partial w}{\partial x} \right)^2 + \left(\frac{\partial v}{\partial z} + \frac{\partial w}{\partial y} \right)^2 \right) \quad (16) \end{aligned}$$

From equation (16) the overall entropy generation rate follows by integration over the flow field volume V :

$$\dot{S}_D = \int_V \dot{S}_D''' dV \quad (17)$$

and from this we immediately get K_E according to equation (15) and thus K when T is set equal to T_∞ .

From now on we assume $T = T_\infty = \text{const}$, so that φ_V in the volume V is

$$\varphi_V = T_\infty \dot{S}_D / \dot{m} \quad (18)$$

With a detailed numerical solution of the flow field in a conduit component, \dot{S}_D''' and thus φ_V according to eqns. (16) to (18) can be determined at a certain Reynolds number.

This method of determining losses can be called *second law analysis* (SLA). It has been validated for the flow in pipes and channels with rough walls by comparing the numerical results with measurements, see [11] and [12] for details.

When V_c is the actual volume of the flow field in the component, φ_{V_c} corresponds to φ_c in equation (12). In order to determine the *additional* losses $\Delta\varphi_u$ and $\Delta\varphi_d$, the difference between φ_V (for the upstream and downstream sections) and those values that hold for the undisturbed flow (no impact of the component) must be found.

With V_u and V_d being the upstream and downstream parts of the flow field (which encounter the influence of the conduit component) the additional specific dissipations are

$$\Delta\varphi_u = \varphi_{V_u} - \varphi_{V_u}^\circ \quad (19)$$

$$\Delta\varphi_d = \varphi_{V_d} - \varphi_{V_d}^\circ \quad (20)$$

Here $\varphi_{V_u}^\circ$ and $\varphi_{V_d}^\circ$ are the specific dissipations in the upstream and downstream volumes V_u and V_d for the undisturbed flow.

Once $\varphi = \Delta\varphi_u + \varphi_c + \Delta\varphi_d$ is known from this procedure for a certain Reynolds number, the loss coefficient K according to equation (1) follows. With several values of $K = K(\text{Re})$ the constants in eqns. (10) and (11) can be determined. Then the Reynolds number dependence of the loss coefficient is known explicitly by eqns. (10) or (11) so that a certain component is characterized by fixed numbers C_1 and C_2 or \hat{C}_1 , \hat{C}_2 and m .

Determination of L_u and L_d is straight forward, based on the definitions (13) and (14), respectively. L_u and L_d will be Reynolds number dependent just like the loss coefficient K itself. Taking into account the flow physics for $\text{Re} \rightarrow \infty$ one can expect that for large Reynolds numbers $L_d/L_u > 1$ will always hold (and increase for increasing Reynolds numbers). When the

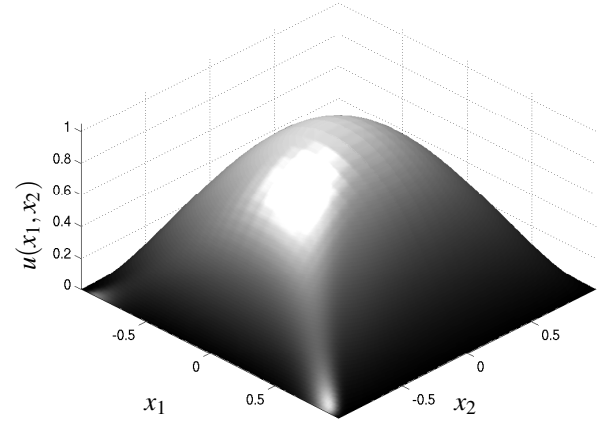


Figure 1. VELOCITY PROFILE OF THE FULLY DEVELOPED LAMINAR FLOW IN A RECTANGULAR CHANNEL NORMALIZED BY ITS MAXIMUM VALUE

component is geometrically symmetric like a 90° bend, for example, $L_d/L_u = 1$ can be expected for $\text{Re} \rightarrow 0$. Then the flow is a creeping flow which is directional independent (the field of streamlines being unchanged when the flow is reversed).

All these presumptions can be proved with the examples given later in this study.

DETAILS OF THE NUMERICAL SOLUTION AND POST-PROCESSING

All calculations described in this paper are performed using the open-source CFD-package OpenFOAM[®] version 1.5. In our approach the NAVIER-STOKES equations for incompressible flow are solved in the finite volume notation. Since the definition of K is only valid for flow developed in time, a steady-state solver is applied. This solver is based on the well known SIMPLE-algorithm for pressure-velocity-coupling and is already part of the OpenFOAM[®]-release. As numerical schemes linear differencing, interpolation, and divergence schemes for pressure, velocity, and related expressions are used. At the inlet analytical velocity profiles for developed laminar flow of a certain Reynolds number are provided, see figure 1 for laminar flow in a rectangular channel. This analytical solution can be found in [5] as a series expansion which here is truncated after a few terms.

Although the determination of losses for the conduit components is based on the steady state solution of the velocity field, it is yet of great interest to determine \dot{S}_D according to equation (17) during the iteration process. Since \dot{S}_D is very sensitive to changes in the flow field, this quantity can be used as an indicator for convergence. Therefore \dot{S}_D and \dot{S}_D''' are explicit results of our calculation available at each pseudo time step.

Numerical grid

Since there are squared gradients in equation (16) it is necessary to compute the velocity field (from which the gradients are determined) with high precision, and local values \dot{S}_D''' have to be adequately resolved to gain all information about the distribution of losses. This leads to a high number of cells used in the computational grid. A grid with a uniform resolution would result in a too large amount of cells and thus would be too expensive. Two possible alternatives are:

- An a priori manual refinement of the grid in areas where high values of \dot{S}_D''' are expected.
- An automatic procedure of adaptive grid refinement in domains with a high local entropy generation \dot{S}_D''' compared to the integral value \dot{S}_D .

All calculations in the following section use automatic grid refinement. Computation is started on an initially block structured grid with nearly cubic cells which are then individually divided into eight new cells with the same aspect ratio as the original cell when a local value $\dot{S}_D''' \cdot dV$ (dV : Volume of a single cell) is larger than a threshold value $c\dot{S}_D$. Here $c = 5 \cdot 10^{-6}$ turns out to be a good compromise between accuracy and computational costs. The refinement procedure is applied several times after a fixed number of iterations is computed following each step of refinement. Refinement stops when no cells exceeding $c\dot{S}_D$ are left. A typical number of cells for a double bend with laminar flow is about 600 000 after the last refinement when symmetry of the flow is assumed.

With this number of cells typical CPU-times are up to 20 hours on a single core of a XEON®-processor, when an algebraic multigrid solver (GAMG) for the pressure equation is used. CPU-times with a preconditioned conjugate gradient solver (PCG) for the pressure turn out to be even higher.

A draw back of this method of grid size minimization is that the geometry of the component approximated by the coarsest grid is not further refined during the calculation. Thus a 90°-bend remains the so called composite mitre bend prescribed by the initial grid, i.e. a bend consisting of several linear sections. According to [5] a slightly increased K-value for this bend could be expected compared to the real smooth bend. This difference can be expected to vanish, however, for a sufficiently large number of initial sections.

Determination of loss characteristics

As a major advantage of the SLA approach it is possible to localize losses exactly at their place of generation. This feature is later used for a simple visualization of loss distribution, see figure 6 below. This information gained by a three dimensional calculation for further application within a one-dimensional approach can be cast into lumped parameters like the K-value in equation (1). In order to get the effect of the conduit component

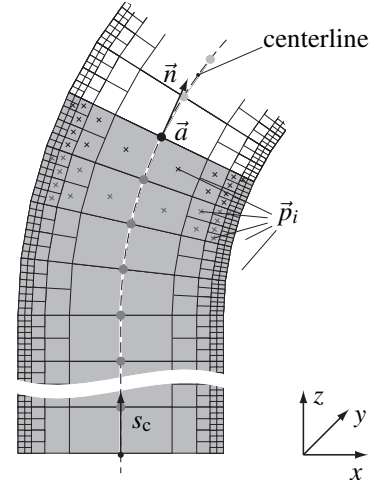


Figure 2. INTEGRATION OF \dot{S}_D''' ALONG THE CENTERLINE OF A CONDUIT COMPONENT AT A CURRENT POINT $s_c = a$; DARK: CELLS WITH CONTRIBUTION TO $[\dot{S}_D]_0^a$

(here: bend) alone, the specific dissipation rates ϕ_{vu}° and ϕ_{vd}° of the fully developed flow in the upstream and downstream parts of the piping system (here: the tangents of a bend) are subtracted.

Determining L_u and L_d also needs an integration of \dot{S}_D''' along the centerline of the conduit component in the direction of the main flow. With s_c as centerline coordinate starting at the inlet, the integral of \dot{S}_D''' over all control volumes with cell centers fulfilling $s_c \leq a$ represents the amount of losses which occur upstream of a plane including point \vec{a} on the centerline with the centerline coordinate $s_c = a$. Points on a common cross section, which is perpendicular to the centerline, have the same value s_c . The integration is done by summing up the values of $\dot{S}_D''' \cdot dV$ for all control volumes i with cell centers \vec{p}_i upstream of a plane perpendicular to the centerline in a point $\vec{a} = [a_x, a_y, a_z]$ on the centerline. With \vec{n} according to figure 2 we get

$$[\dot{S}_D]_0^a = \sum_I \dot{S}_{DI}''' \cdot dV_I, \text{ with } I = \{i \in \mathbb{N} | (\vec{p}_i - \vec{a}) \cdot \vec{n} < 0\} \quad (21)$$

If a cutting plane intersects the centerline in more than one point, e.g. in case of a 180°-bend, the set I in equation (21) has to be slightly modified for a correct integration. Integration according to equation (21) is done for a number of points \vec{a} in advance so that it is possible to interpolate between these discrete values of $[\dot{S}_D]_0^{s_c} = \dot{S}_D(s_c)$. Points \vec{a} at which equation (21) is evaluated belong to the initial unrefined grid to ensure that no cells are divided by the cutting plane. This limits the amount of sampling points according to the coarsest resolution in streamwise direction, see figure 2.

With integration up to a second point \vec{b} , it is possible to de-

termine the losses between two distinct cross sections of the conduit component. With \vec{a} at the exit of the component, e.g. at the beginning of the downstream tangent of a bend, and \vec{b} at a variable location downstream of \vec{a} it is possible to compute L_d as follows:

- In a first step \vec{b} is set to the maximum value, i.e. to the exit of the computational domain. From $[\dot{S}_D]_a^b$, the value of the entropy generation rate of an undisturbed flow in a channel of a length equal to the distance from \vec{a} to \vec{b} is subtracted. If the computational domain is sufficiently large this remaining value represents the amount of additional entropy generation caused by the component, i.e. the entropy generation rate corresponding to $\Delta\phi_d$. The entropy generation for the undisturbed flow could be a value from an analytical solution or better, for reasons of model consistency, a value extracted from the numerical solution, see equation (22) below.
- In a second step \vec{b} is varied systematically to determine the position \vec{b}_{L_d} at which 95 % of the downstream losses (corresponding to $0.95\Delta\phi_d$) are reached. The downstream length L_d then is the distance between \vec{a} and \vec{b}_{L_d} .

The upstream length L_u is determined in a similar way. The additional losses in the upstream and downstream parts of the conduit provide the specific dissipations $\Delta\phi_u$ and $\Delta\phi_d$, respectively, using an equation analogous to equation (18). These specific dissipations, referred to the total dissipation ϕ_c induced by the component, are displayed in component specific tables according to table 2.

With $\dot{S}_D(s_c)$ known it is illustrative to compute its derivative $\dot{S}'_D = d\dot{S}_D/ds_c$ and thus show the distribution of losses. For a fully developed channel flow $\dot{S}'_D(s_c)$ is constant. This occurs far upstream and far downstream of the component, where this values (\dot{S}'_D) can be compared to analytical solutions for developed laminar channel-flow to validate the calculation. Multiplication of \dot{S}'_D with the length of the upstream or downstream tangents and then using equation (18) yields $\phi_{V_u}^o$ or $\phi_{V_d}^o$, respectively, i.e.

$$\phi_{V(u,d)}^o = \dot{S}'_D L_{V(d,u)} T / \dot{m} \quad (22)$$

Normalizing $\dot{S}'_D(s_c)$ with \dot{S}'_D^o (undisturbed flow), values of $\dot{S}'_D(s_c)/\dot{S}'_D^o$ differing from 1 indicate the influence of the component on the fully developed flow, see figures 5 and 6 below.

Note that ds_c in the derivative is represented by the EUCLIDIAN distance Δs_c of two adjacent points on the centerline, see figure 2. In straight parts of the component Δs_c gives the increase in volume $\Delta V = A(s_c)\Delta s_c$, when A is the cross sectional area. In curved parts of the component $\Delta V = A(s_c)\Delta s_c$ is still valid for geometries with rectangular cross sections, due to the prismatic shape of the additional volumes or the GULDINUS theorem in case of a continuous approach, which computes the volume of a

solid of revolution as the product of the cross sectional area and the path traveled by its centroid. This allows a direct comparison of straight and curved sections for certain geometries.

For the special situation of creeping flow in a bend it turns out that losses per length are smaller in a section of the curved geometry than in the straight sections, see figure 5. The mass flow predominantly is near the inner parts of the bend where losses are lesser since the effective passage length is shorter.

Empirical correlations for K

As already mentioned it is very convenient to provide the K-value for a certain component as a function of the Reynolds number in the form of an empirical equation which is easy to use, see the ansatz functions $K(C, Re)$ in eqns. (10) and (11). Here the constants ($C = [C_1, C_2]$ for the simple blending or $C = [\hat{C}_1, \hat{C}_2, m]$ following CHURCHILL and USAGI) are computed with the help of least squares optimization. A direct fit of $K(C, Re)$ to the values $K(Re)$ obtained from the numerical model would lead to an unsatisfactory result, because the fit would be best for the highest values of K. High K-values are for small Reynolds numbers where the losses are actually lower than for high Reynolds numbers. To increase the accuracy of the least squares fit for small K-values at high Reynolds numbers (where the highest losses occur), we normalize the target function with the values of K. This leads to the following equation to be solved, e.g. by MATLAB[®], with C as solution.

$$\sum_i \left(\frac{K(C, Re_i)}{K(Re_i)} - 1 \right)^2 \stackrel{!}{=} \min \quad (23)$$

EXAMPLES

The method for determining K of a certain conduit component is applicable to all kinds of components. Indeed there is a large variety of components like bends, junctions, diffusors, nozzles, ... all with one or often more than one intrinsic geometrical parameter like aspect ratio, radius of curvature, area ratio, Altogether there are probably hundreds of special geometries of interest. For turbulent flows the situation is quite similar and the large number of special geometries reflects itself in the comprehensive collections [4] and [5] mentioned in the introduction already.

Since each single component affects the flow field not only within its own geometry but leads to an upstream and downstream length of influence (introduced as L_u and L_d in equations (13) and (14)) there is a special problem when a second component follows too closely downstream. Only when the distance between two components is larger than the sum of L_d of the first and L_u of the second component their K-values can be added to

describe the effect of both components together. When the distance is shorter, there are two options:

- one nevertheless takes $K_1 + K_2$ as the K-value for both components (with the same u_m , c.f. equation (5)) accepting an unknown error through this procedure.
- both components are treated as one new component for which K is determined like for all single components.

The second option obviously is the more reliable one. It, however, increases the number of single components that have to be treated individually considerably.

On the background of the general problem (large number of single components and unknown effects of component-combinations) just to demonstrate the method we restrict ourselves to four specific examples: one single 90° bend and three different combinations of two such bends, all with the same aspect ratio and the same radius of curvature. The question, how good the double bends are described by twice the K-value of the single bend, is of special interest.

Single 90° bend

Figure 3 shows the geometry of a 90° bend with a quadratic cross section $A = D_h^2$ and a curvature radius $r = D_h$. For the numerical solutions the straight channels upstream and downstream of the bend are long enough to determine L_u and L_d according to equations (13) and (14) for all Reynolds numbers under consideration ($4 \leq Re \leq 512$). Applying all the numerical details described in the previous chapter we get the results in table 3 which in its form is in accordance to the general table 2. Based on the extended ansatz (11) for the K-value we find K_{90° for the single 90° bend to be

$$K_{90^\circ} = [2.20^{2.19} + (88.98/Re)^{2.19}]^{1/2.19} \quad (24)$$

In figure 4 this curve is shown together with the individual points to which it is fitted.

It is interesting to note how the entropy generation and thus the (additional) losses are distributed in streamwise direction. In figure 6 this distribution is shown for a small and a large Reynolds number ($Re = 4$ and $Re = 512$).

The following aspects are worth to be mentioned:

- Losses in absolute values increase with increasing Reynolds numbers (“though” the K-values decrease). For example, according to equation (1), the specific dissipation is $\varphi = 3.99 \text{ m}^2/\text{s}^2$ for $Re = 4$ ($D_h = 100 \mu\text{m}$, fluid: air with $\nu = 15 \cdot 10^{-6} \text{ m}^2/\text{s}$) but $6695 \text{ m}^2/\text{s}^2$ for $Re = 512$, i.e. about 1677 times larger. This is reflected in the strong increase of the gray area in figure 6(a) compared to figure 6(b).

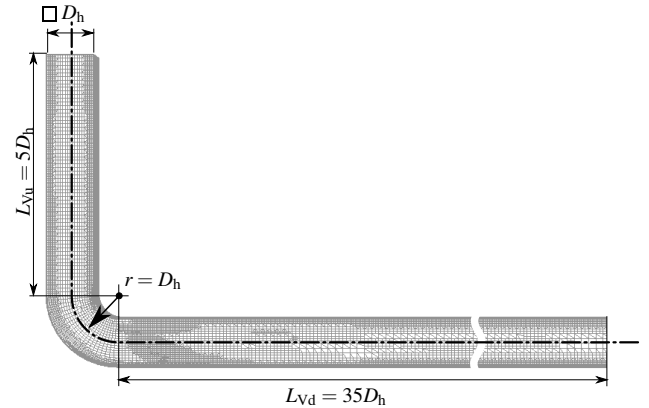


Figure 3. GEOMETRICAL DETAILS OF THE 90° BEND OF THIS STUDY

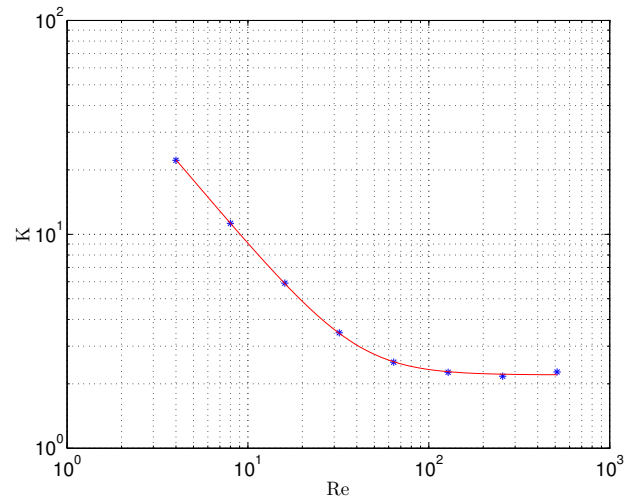
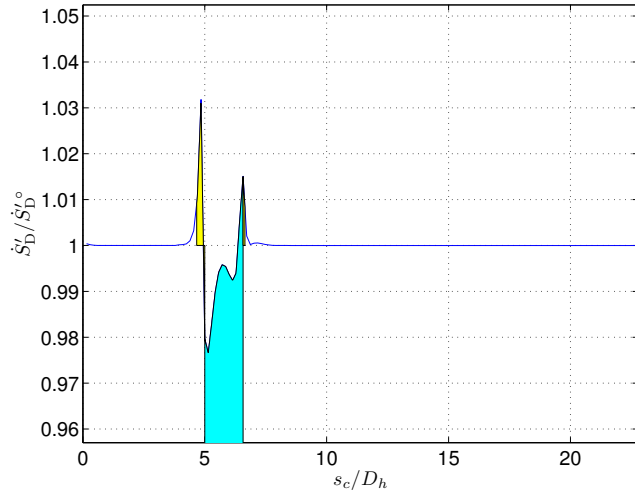


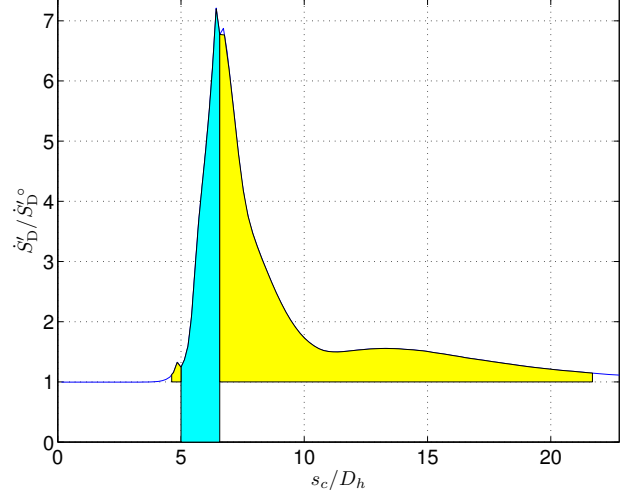
Figure 4. LOSS COEFFICIENT K FOR THE 90° BEND; *: RESULTS, TABLE 3; —: ANSATZ (24)

Table 3. DETAILED INFORMATION ABOUT LOSSES DUE TO A 90° BEND; CROSS SECTION: $A = D_h^2$, CURVATURE RADIUS: $r = D_h$

Re	$\Delta\varphi_u/\varphi$	φ_c/φ	$\Delta\varphi_d/\varphi$	L_u/D_h	L_d/D_h	K
	eqn. (12)	eqn. (12)	eqn. (12)	eqn. (13)	eqn. (14)	eqn. (1)
4	(0.0045)	0.9954	(0.0001)	(0.3320)	(0.0779)	22.19
8	(0.0066)	0.9913	(0.0022)	(0.4048)	(0.4347)	11.25
16	0.0097	0.9727	0.0176	0.4505	0.9091	5.91
32	0.0127	0.8985	0.0888	0.5183	1.3720	3.46
64	0.0130	0.7262	0.2609	0.5724	2.1634	2.53
128	0.0104	0.5367	0.4529	0.6147	3.4676	2.26
256	0.0077	0.4029	0.5894	1.0797	8.3494	2.17
512	0.0040	0.2859	0.7101	0.3791	15.1179	2.27



(a) Re=4



(b) Re=512

Figure 6. DISTRIBUTION OF THE CROSS-SECTIONAL ENTROPY GENERATION RATE \dot{S}'_D/\dot{S}'_D^o IN STREAMWISE DIRECTION IN A 90° BEND; \dot{S}'_D : ENTROPY GENERATION RATE FOR THE FULLY DEVELOPED FLOW; DARK GRAY: ENTROPY GENERATION IN THE 90° BEND; LIGHT GRAY: ENTROPY GENERATION UPSTREAM AND DOWNSTREAM OF THE 90° BEND

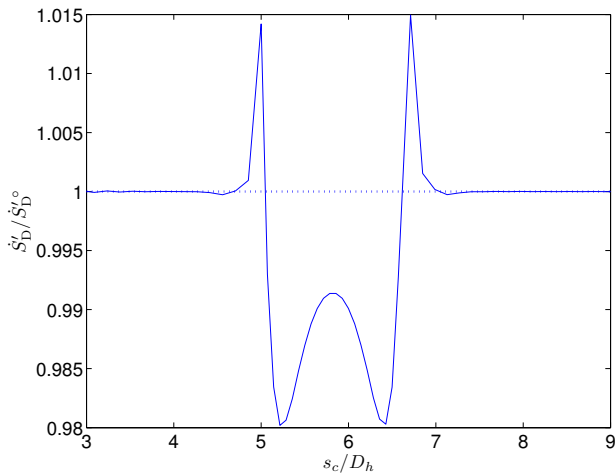


Figure 5. DISTRIBUTION OF THE CROSS-SECTIONAL ENTROPY GENERATION RATE \dot{S}'_D/\dot{S}'_D^o IN STREAMWISE DIRECTION FOR CREEPING FLOW ($Re = 0$) IN A 90° BEND

- For low Reynolds numbers almost all losses occur in the 90° bend itself with little additional dissipation upstream and downstream of the bend. This, however, is very different for high Reynolds numbers, where more and more of the losses due to the bend occur downstream. For $Re = 512$, for example, 71 % are additional losses in the flow field downstream characterized by the downstream length L_d which is ≈ 15 times the hydraulic diameter.
- For $Re \rightarrow 0$ the flow field is that of a creeping flow. In a streamwise symmetrical geometry (like the 90° bend) the

flow field then is symmetrical, too, with the consequence that $L_u = L_d$ should hold. In table 3 the values of L_u and L_d are very different and approach each other for smaller values of Re . Since, however, both lengths are very small for $Re \rightarrow 0$ and hardly any additional dissipation occurs outside the bend, numerical uncertainties more and more dominate the determination of L_u and L_d (which are of no practical importance for $Re \rightarrow 0$). Results for these cases are given in brackets.

The perfect symmetry of the flow field in the limit $Re \rightarrow 0$ is nevertheless shown in figure 5 where $Re = 0$ is set for the determination of \dot{S}'_D/\dot{S}'_D^o .

90° bend combinations

Figure 7 shows the geometry of three different combinations of two 90° bends (described in the previous sub-chapter), together with the final results with respect to the K-values for these combinations. All tables according to the model-table (table 2) can be found in the appendix. Here, we only want to compare the K-values for various Reynolds numbers. This is done in table 4 where the K-values of the double bend combinations are compared to $2K_{90^\circ}$, i.e. twice the K-value of the single bend.

There is a clear trend: As long as losses occur predominantly within the geometry, $2K_{90^\circ}$ is a good approximation to the individual K-values of the various combinations of two 90° bends. This is the case for small Reynolds numbers. If we again use a 95 % criterion (like with the determination of L_u and L_d) table 3 for the single bend shows that for $Re \leq 16$ more than 95 % of the losses occur in the bend itself. This corresponds to the fact

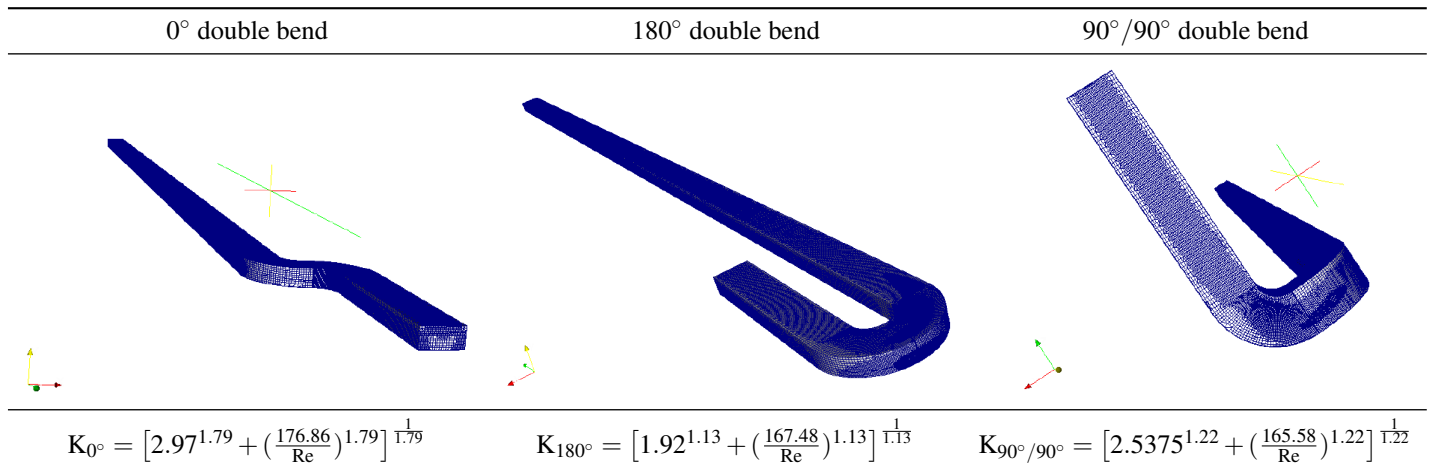


Figure 7. GEOMETRY AND K-VALUES OF DOUBLE BEND COMBINATIONS; SEE FIGURE 3 FOR THE SINGLE BEND

Table 4. COMPARISON OF K-VALUES FOR THREE DIFFERENT 90° BEND COMBINATIONS WITH TWICE THE K-VALUE OF A SINGLE 90° BEND

Re	2 × 90° bend	0° double b.	180° double b.	90°/90° double b.
4	44.38	43.76	43.76	43.51
8	22.50	22.20	22.14	22.05
16	11.82	11.67	11.57	11.59
32	6.93	6.71	6.63	6.76
64	4.51	4.35	4.31	4.60
128	4.53	3.15	3.06	3.53
256	4.34	3.06	2.31	2.90
512	4.54	3.18	2.20	2.68

that for all three 90°-combinations and $Re \leq 16$ the individual K-values are close to each other and also close to $2K_{90^\circ}$. For higher Reynolds numbers, however, K-values differ appreciably. If, for example, the K-value for the 180° double bend at $Re = 512$ is approximated by the corresponding value for $2K_{90^\circ}$ there is an error of more than 100 %.

As a general trend K-values of the combinations are lower than $2K_{90^\circ}$ since for high Reynolds numbers large parts of the losses occur downstream of the components. This happens twice for two single bends, but once only when two bends are combined to one single component. This should carefully be taken into account when flow systems are designed on the basis of individual K-values of standard conduit components.

DISCUSSIONS

Loss coefficients are introduced based on some explicit and some implicit assumptions. Two important aspects, incompress-

ibility and the temperature level, will be finally discussed.

Check of the incompressibility-assumption

In equation (2) and equation (5) it was assumed that the flow is incompressible, i. e. that $\rho = \text{const}$ holds. For a gas, however, there may be considerable changes in ρ when large pressure differences Δp occur in conduit components of micro size.

If a 5 % density change $\Delta\rho/\rho = 0.05$ is accepted this corresponds to the same amount of change in pressure when the fluid is an ideal gas and $T = \text{const}$ is assumed (then $\rho = (RT)^{-1} \cdot p$ holds)

For a conduit component with $u_{m1} = u_{m2}$ the total head loss is equal to the pressure difference Δp , so that equation (5) can be used for K. Together with the Reynolds number we get

$$\Delta p = \frac{K Re \mu u_m}{2 D_h} \quad (25)$$

Accepting a 5 % change in pressure (and thus density) this leads to

$$\frac{\Delta p}{p} = \frac{K Re \mu u_m}{2 p D_h} \leq 0.05 \quad (26)$$

or with $\mu = \rho \nu$ and the ideal gas law $p/\rho = RT$ to

$$D_h \geq 10 K Re \frac{\nu u_m}{RT} \quad (27)$$

From this condition the threshold value for D_h follows, which, however, is very small when typical numbers for Re , ν , u_m , R ,

and T are assumed. For example, with $Re = 100$, i. e. $K = 4$ for a 90° bend, $\nu = 15 \cdot 10^{-6} \text{ m}^2/\text{s}$, $R = 287 \text{ J/kgK}$, $u_m = 0.1 \text{ m/s}$ and $T = 300 \text{ K}$ the “incompressibility condition” for D_h is $D_h \geq 7 \cdot 10^{-8} \text{ m} = 0.07 \mu\text{m}$ which for all MEMS applications will be fulfilled.

Dissipation and entropy generation

In the section “THERMODYNAMIC CONSIDERATIONS” it was shown that dissipation is completely equal to an exergy loss only for $T = T_\infty$. At temperature levels $T > T_\infty$, for example, the dissipated energy $\dot{m}\phi_V$ corresponds to a lost exergy $\dot{m}\phi_V T_\infty/T$ only. The reason for this reduced exergy loss is, that in the dissipation process mechanical energy is converted into internal energy. For $T > T_\infty$, however, this internal energy has a non-zero exergy fraction, and thus not the whole of $\dot{m}\phi_V$ is “lost”.

From eqns. (15) - (18) it follows that for $T \neq T_\infty$ and $T = \text{const}$, K_E and K are linked by

$$K = \frac{T}{T_\infty} K_E \quad (28)$$

which clearly illustrates the influence of the temperature level which is not accounted for by a purely fluid mechanical definition of the head loss coefficient in equation (1).

CONCLUSIONS

Loss coefficients for conduit components (here: in the laminar flow regime) can be found by determining the local entropy generation rates due to the dissipation of mechanical energy (second law analysis, SLA) at $T = T_\infty$. In addition to the coefficient itself this also gives detailed information about the distribution of losses in the flow field. Determination of the upstream and downstream lengths of influence is important when single conduit components should be combined, still using loss coefficients of the undisturbed single components. What has been shown here for some conduit components can likewise be applied for all other components of special or general interest, and of course can be extended to turbulent flows.

APPENDIX: LOSS-DETAILS OF 90° BEND COMBINATIONS

Table 5. DETAILED INFORMATION ABOUT LOSSES DUE TO A 0° DOUBLE BEND; CROSS SECTION: $A = D_h^2$, CURVATURE RADIUS:

$r = D_h$						
Re	$\Delta\phi_u/\phi$	ϕ_c/ϕ	$\Delta\phi_d/\phi$	L_u/D_h	L_d/D_h	K
4	(0.0018)	0.9979	(0.0003)	(0.2886)	(0.0895)	43.76
8	(0.0028)	0.9958	(0.0014)	(0.3346)	(0.5963)	22.19
16	0.0044	0.9857	0.0099	0.4323	0.9793	11.67
32	0.0060	0.9466	0.0474	0.4865	1.4757	6.71
64	0.0071	0.8895	0.1033	0.5896	2.6150	4.35
128	0.0073	0.8767	0.1160	0.7330	2.2102	3.15
256	0.0051	0.7157	0.2791	0.6414	8.8529	3.06
512	0.0034	0.5215	0.4751	0.6782	15.2465	3.18

Table 6. DETAILED INFORMATION ABOUT LOSSES DUE TO A 180° DOUBLE BEND; CROSS SECTION: $A = D_h^2$, CURVATURE RADIUS: $r = D_h$

$r = D_h$						
Re	$\Delta\phi_u/\phi$	ϕ_c/ϕ	$\Delta\phi_d/\phi$	L_u/D_h	L_d/D_h	K
4	(0.0018)	0.9979	(0.0003)	(0.2890)	(0.0863)	43.76
8	(0.0029)	0.9959	(0.0012)	(0.3355)	(0.5755)	22.14
16	0.0046	0.9875	0.0079	0.4344	0.9590	11.57
32	0.0065	0.9589	0.0347	0.4872	1.3383	6.63
64	0.0077	0.9100	0.0823	0.5885	2.1063	4.31
128	0.0080	0.8634	0.1286	0.7407	3.4604	3.06
256	0.0072	0.8223	0.1705	0.6738	4.4154	2.31
512	0.0045	0.6467	0.3488	0.4234	16.2145	2.20

Table 7. DETAILED INFORMATION ABOUT LOSSES DUE TO A $90^\circ/90^\circ$ DOUBLE BEND; CROSS SECTION: $A = D_h^2$, CURVATURE RADIUS: $r = D_h$

$r = D_h$						
Re	$\Delta\phi_u/\phi$	ϕ_c/ϕ	$\Delta\phi_d/\phi$	L_u/D_h	L_d/D_h	K
4	(0.0017)	0.9982	(0.0001)	(0.2531)	(0.0483)	43.51
8	(0.0027)	0.9963	(0.0010)	(0.3116)	(0.5428)	22.05
16	0.0043	0.9871	0.0086	0.3822	0.9521	11.59
32	0.0060	0.9512	0.0429	0.4607	1.3661	6.76
64	0.0068	0.8793	0.1139	0.5633	2.2560	4.60
128	0.0066	0.8013	0.1922	0.6514	4.3956	3.53
256	0.0056	0.7347	0.2597	0.6622	9.7026	2.90
512	0.0037	0.6143	0.3819	0.4977	19.8843	2.68

REFERENCES

- [1] Munson, B., Young, D., and Okiishi, T., 2005. *Fundamentals of Fluid Mechanics*, 5th ed. John Wiley & Sons, Inc., New York.
- [2] White, F., 2008. *Fluid Mechanics*, 6th ed. McGraw-Hill, New York.
- [3] Herwig, H., 2008. *Strömungsmechanik*. Vieweg+Teubner Verlag, Wiesbaden.
- [4] Idelchik, I., 1986. *Handbook of Hydraulic Resistance*. Hemisphere Publ. Corp., New York.
- [5] Ward-Smith, A. J., 1980. *Internal Fluid Flow*. Clarendon Press, Oxford.
- [6] Herwig, H., and Wenterodt, T., 2009. “Wall roughness effects: A second law analysis (SLA)”. In Proceedings of the IUTAM symposium on the physics of wall-bounded flows on rough walls, Cambridge, GB.
- [7] Churchill, S. W., and Usagi, R., 1974. “A standardized procedure for the production of correlations in the form of a common empirical equation”. *Ind. Eng. Chem. Fundamen.*, **13**, pp. 39–44.
- [8] Bejan, A., 1996. *Entropy Generation Minimization*. CRC Press, Boca Raton.
- [9] Herwig, H., and Wenterodt, T., 2008. “The role of entropy production in momentum and heat transfer”. In 7th International Symposium on Heat Transfer (ISHT7), Beijing, China.
- [10] Herwig, H., and Kautz, C., 2007. *Technische Thermodynamik*. Pearson Studium, München.
- [11] Gloss, D., and Herwig, H., 2009. “Micro channel roughness effects: a close-up view”. *Heat Transfer Engineering*, **32**, pp. 62–69.
- [12] Gloss, D., and Herwig, H., 2010. “Wall roughness effects in laminar flows: An often ignored though significant issue”. *Exp. in Fluids (online first)*, DOI 10.1007/s 00348-009-0811-6.